Int. J. Electrochem. Sci., 11 **(2016)** 3074 - 3085

International Journal of
ELECTROCHEMICAL
SCIENCE
www.electrochemsci.org

Synthesis of Magnetite/ Hematite/ Iron Nanocomposites by the Low Voltage Arc Discharge in Water in the Presence of External Magnetic Field

Hassan Karami[1,2,*], *Fariba Goli*[1], *Juliet Ordoukhanian*[1]

[1] Department of Chemistry, Payame Noor University, 19395-4697, Tehran, I.R. of Iran
[2] Nano Research Laboratory, Department of Chemistry, Payame Noor University, Abhar, I.R. of Iran
[*]E-mail: karami_h@yahoo.com

Received: 10 September 2015 / *Accepted:* 12 October 2015 / *Published:* 1 March 2016

A new method for the synthesis of magnetite/ hematite/ iron nanocomposites (MHINC) is introduced. In this method, a low-voltage arc is discharged between two iron electrodes in distilled water while an external magnetic field with the nominal power of 0.4-1.6 T is applied during synthesis. The measured magnetic field exactly on the anode tip is 80 to 210 mT. By arc discharge, iron is oxidized to iron oxides. The synthesized samples are characterized by SEM, TEM, XRD and VSM techniques. The sizes distributions of some samples are identified by dynamic light scattering (DLS) test. The obtained results show the presence of the external magnetic field can decrease the particle sizes and also increases the saturation of magnetization and the transformation rate of iron into iron oxide in nanocomposite.

Keywords: External magnetic field; Arc discharge; Nanocomposite; Iron; Magnetite; Hematite

1. INTRODUCTION

Iron- based nanomaterials are mainly consisted of zero valent iron and iron oxides. The most common oxides are magnetite (Fe_3O_4), hematite (α-Fe_2O_3) and maghemite (γ-Fe_2O_3). Magnetite is a ferromagnetic material and has the strongest magnetism between iron oxides. Hematite is weakly ferromagnetic and extremely stable at ambient conditions. Maghemite also has a few ferromagnetic properties and metallic iron is fully ferromagnetic. Characteristics of these iron oxides are mostly the trivalent state of iron, low solubility, relatively low toxicity and biodegradability.

Magnetic iron oxide nanocomposites have shown the distinctive chemical, catalytic, electronic and magnetic properties. These unique properties have been so beneficial for a wide range of scientific

and technical applications, including catalyst for many chemical reactions [1], gas sensors [2], semiconductors [2], pigments [3] and coatings [4], magnetic recording [5], magnetic data storage devices [6], toners and inks for xerography [7], magnetic resonance imaging [8], wastewater treatment [9], bioseparation [9] and targeted drug delivery in medicine[10, 11].

Magnetic properties such as saturation magnetization are known to be closely related to the morphology and size of magnetic materials and narrow particle size distribution is one of the imperatives of their synthesis [12-14].

Different methods have been proposed for the synthesis of iron oxide nanocomposites, like hydrothermal reactions [15], chemical precipitation [16], Chemical vapor deposition [17], microemolusion [18], sol-gel synthesis [19], solid phase pyrolysis [20] and electrochemical deposition [21]. Karami et. al. (2013) reported a simple and low cost method for the synthesis of iron oxide nanocomposites by low voltage arc discharge method in aqueous media [22]. Recently, some syntheses have done in the presence of an external magnetic field which affected the growth size and composition of iron synthesized nano structures [23-26].

Sano et al published two paper about the arc discharge between two carbon electrodes in water as a new technique to synthesize carbon nanomaterials [27,28]. Fan et al in 2007 used arc discharge between graphite cathode and iron anode in water to synthesize magnetite nanoparticles in large scale [29]. Wang et al reported the arc discharge between iron filaments in sodium chloride solution to synthesize magnetite powder [30]. In the current work, we used arc discharge between two iron electrodes in water to synthesize magnetite/ hematite/ iron nanocomposite (MHINC) in the presence of an external magnetic field. The prepared nanocomposites were characterized by Transmission Electron Microscopy (TEM), X-Ray Diffraction (XRD), Scanning Electron Microscopy (SEM), Dynamic light Scattering (DLS) and Vibrating Sample Magnetometer (VSM) techniques. As it was expected, magnetic field decreases the grain size of nanocomposites and led to more homogeneity in the distribution of phases in nanocomposites [31].

2. EXPERIMENTAL

2.1. Materials

The presented method is a green chemical synthesis method and requires no chemicals. Only distilled water was used in all experiments. Two iron electrodes with a narrow bent tip used very close together to make the electrical arc in distilled water media.

2.2. Instruments

A 30 V- 10 A power supply (made in China) was coupled with a 50 V- 10 A power supply (made in china) in series in order to provide the required voltage for the arc. The external magnetic field is supplied by using 0.4 T rectangular cube (7cm×5cm×2cm) permanent NdFeB magnets arranged in parallel and perpendicular positions to the surface of electrodes, which superimpose

magnetic fields of 80 to 210 mT measured using home-made Gauss meter exactly on the anode tip. The temperature of the solution was kept constant in a Pars Azma water bath (Iran). The structures of the synthesized nanocomposites were characterized by XRD Shimadzu 6000 used Cu (K_α) incident radiation. The TEM P(hilips EM208) and the SEM (Hitachi 4160) were used to determine the morphology and the particle size. The saturation magnetization of nanoparticles was determined by the VSM Lake Shore 7200 from USA. Size distribution diagrams of the samples were obtained by DLS (Malvern, Zetasizer Nano ZS3600).

2.3. Synthesis procedure

Synthesis of MHINC was performed in the set up of electric arc between two iron electrodes immersed in 150 ml distilled water at the temperature of 40 °C. It should be noted that with the establishment of an arc, the temperature can rise locally to 3500 °C but, by putting the electrochemical cell in a water bath, the solution temperature is kept constant at 40 °C. However, when the temperature reached over 40 °C, the synthesis is stopped to drop. The tips of the electrodes were placed facing each other with a gap of 1 mm.

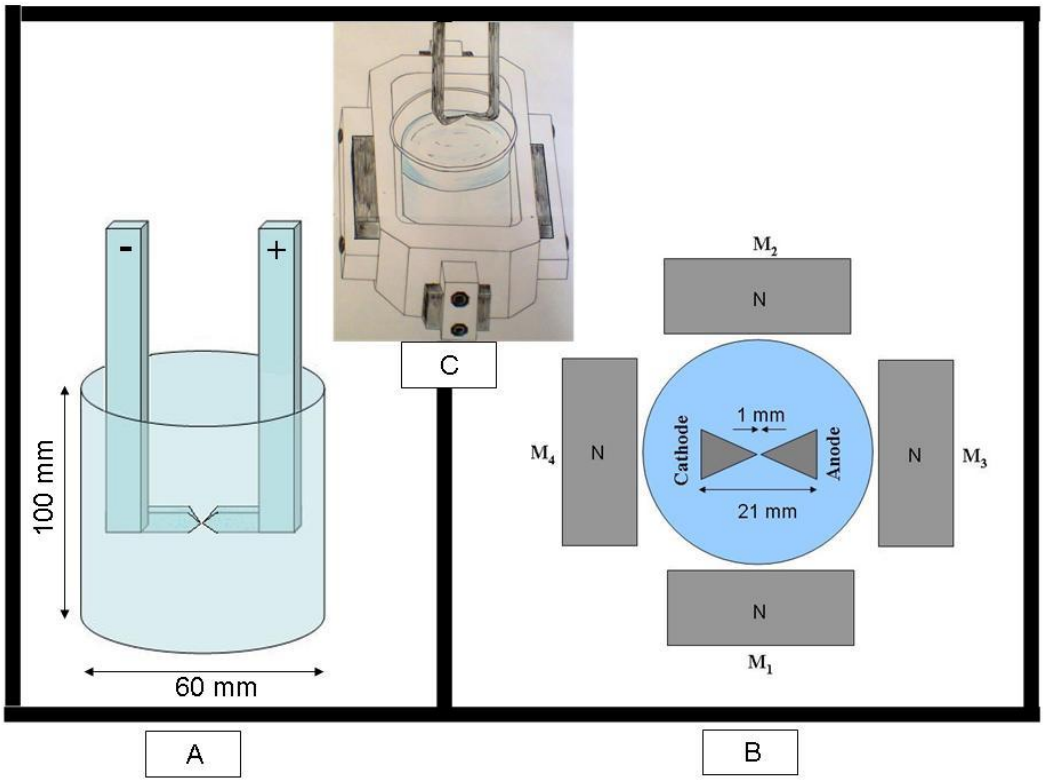

Figure 1. Experimental set up for MHINC synthesis; Electrochemical cell (A), magnets Array (B) and image of the experimental setup (C).

The arc chamber was put in the assembled magnetic field device (Fig. 1). The dimensions of electrodes are also shown in Fig. 1. In 0.4- 1.6 T magnetic field MHINC samples were synthesized by

anodic oxidation of iron electrode. I all experiments, the power supply provides average 80 V dc voltage between anode and cathode tubes with the average operating current of 1 A. During arc discharge, some iron is plucked from the electrode tip and the magnetite/ hematite/ iron nanocomposite is formed. When the synthesis was completed (average synthesis time was 30 min), the reaction solution was heated to 90°C then, the nanocomposite precipitation was separated from solution by the membrane filtration (Cellulose acetate membrane with pore diameter of 0.45 μ). Finally, the filtered sample is dried at ambient temperature. The prepared nanopwder was analyzed by SEM, XRD, TEM and DLS. All experiments were conducted at atmospheric pressure.

3. RESULTS AND DISCUSSION

Synthesis of MHINC samples was done as described in section 2.3. To investigate the effects of external magnetic field, five syntheses were performed. First synthesis was done without any magnetic field. Second synthesis was performed in the presence of one 0.4 T magnet. In next experiments, two, three and four magnets (each magnet is 0.4 T) were used, respectively. The effects of magnetic fields, applying during synthesis of MHINC have studied in five conditions as followings:

S_1: Synthesis without magnetic field

S_2: Synthesis in the presence of one vertical magnet parallel to the electrodes (Nominal magnetic field is 0.4 T and the measured magnetic field on the surface of anode tip is 80 mT)

S_3: Synthesis in the presence of two vertical magnets on both sides of electrodes (Nominal magnetic field is 0.4 T and the measured magnetic field on the surface of anode tip is 150 mT)

S_4: Synthesis in the presence of two vertical magnets on both sides of electrodes and third magnet in the horizontal position perpendicular to the two previous magnets (Nominal magnetic field is 0.4 T and the measured magnetic field on the surface of anode tip is 180 mT)

S_5: Synthesis in the presence of two vertical magnets on both sides of electrodes and third and fourth magnets in the horizontal positions and perpendicular to the two previous magnets (Nominal magnetic field is 0.4 T and the measured magnetic field on the surface of anode tip is 210 mT)

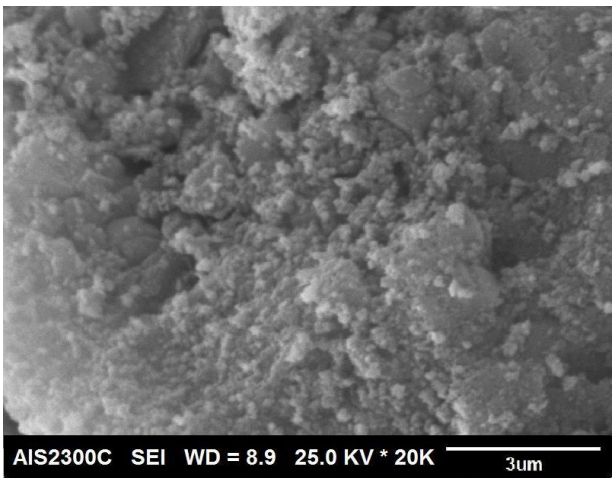

A

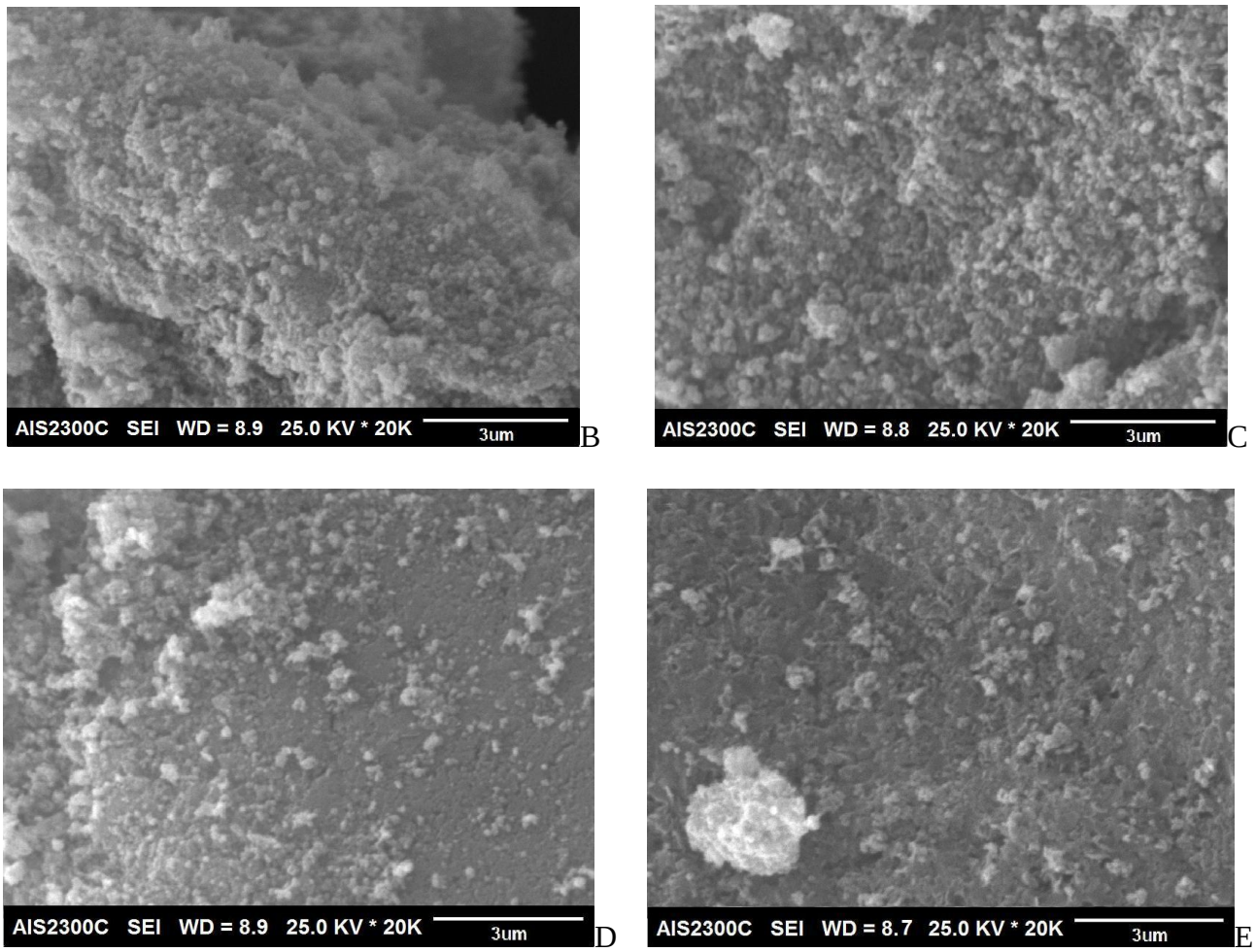

Figure 2. SEM images of MHINC samples synthesized in the presence of different magnetic fields; (a) without magnetic field, (b) 0.4 T, (c) 0.8 T, (d) 1.2 T, and (e) 1.6 T magnetic field.

SEM images provide the information about the size and shape of the synthesized samples. Figure 2 Shows the SEM images of MHINC samples synthesized in the above mentioned conditions, which indicate that some samples consisted of nano- scale particles with uniform distribution. All particles have the same spherical morphology.

All SEM images were analyzed by Microstructure measurement software to determine the average particles sizes. The calculated data were summarized in Table 1.

Table 1. SEM and DLS data for size distribution and the average particles sizes of the fives MHINC samples synthesized under different magnetic field power.

Synthesis	Number of magnets	Particles size Distribution (NM)		Average Particle size (NM)	
		SEM	DLS	SEM	DLS
S_1	0	120-160	110-148	140	128
S_2	1	70-110	71-95	90	82
S_3	2	65-90	53-82	87	66
S_4	3	5-20	1-13	12	7
S_5	4	5-22	1-13	13	8

To confirm the calculated particles sizes based on SEM images, all samples were examined by DLS technique (Fig. 3). All data of DLS diagrams for the size distribution of five synthesized samples were shown in Table 1 to compare with SEM results. As can be seen in Table 1, by increasing the number of magnets, the average particles sizes is reduced considerably. The results in the presence of 3 and 4 magnets are not different. Therefore, applying a nominal magnetic field of 1.2 T (3 magnets) to achieve the narrow range and the smallest average particle size is sufficient.

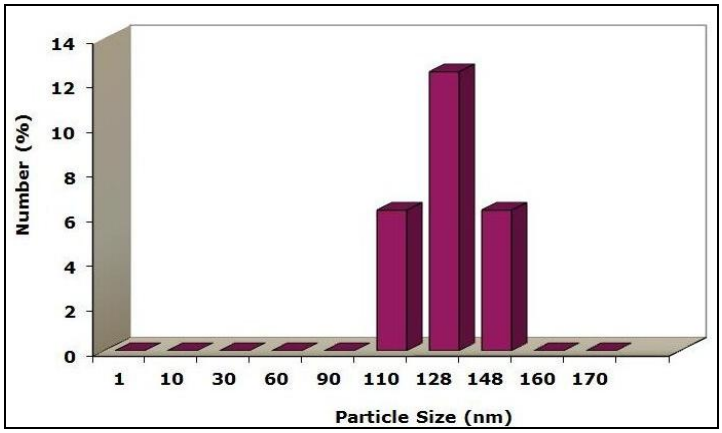

(S_1)

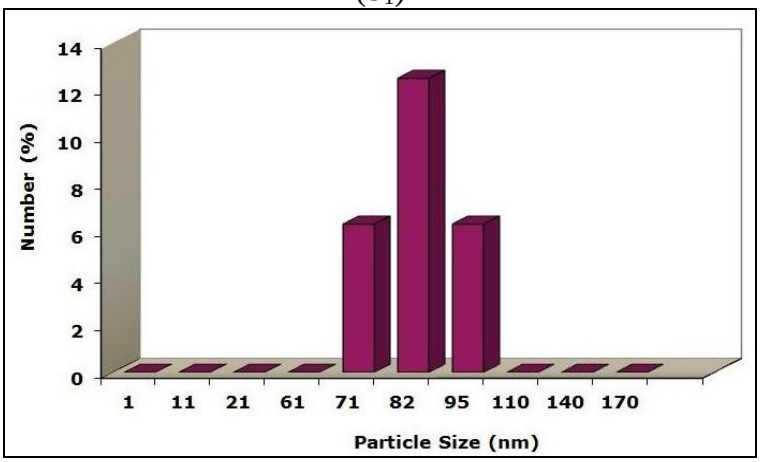

(S_2)

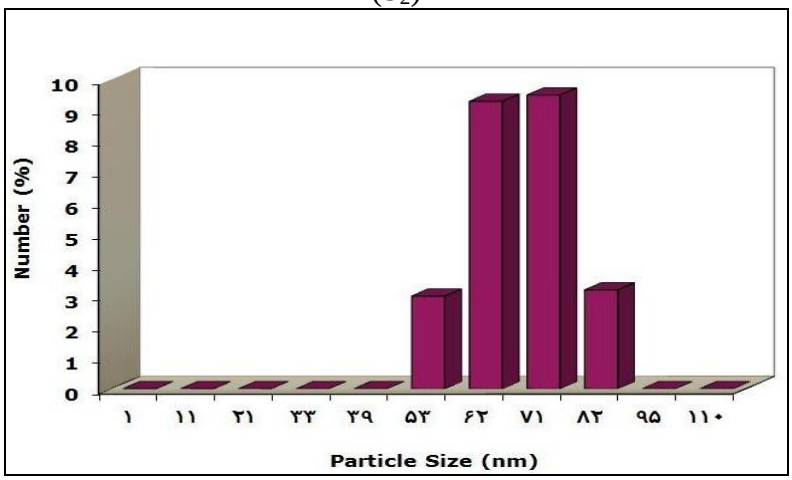

(S_3)

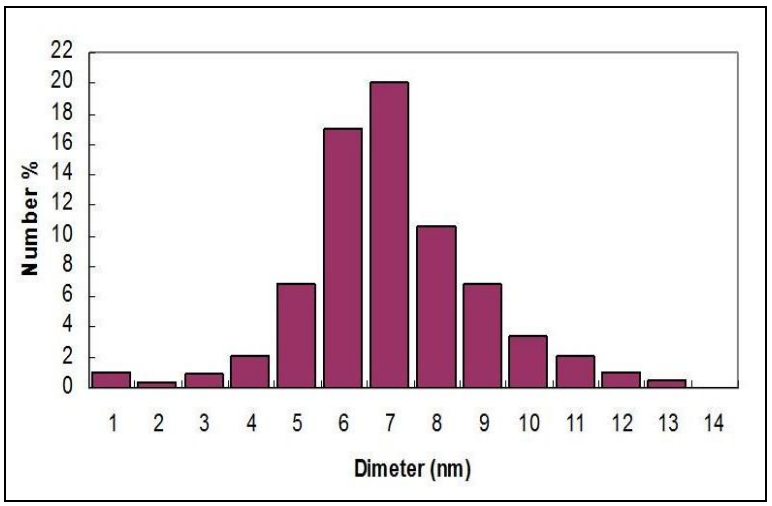

(S_4)

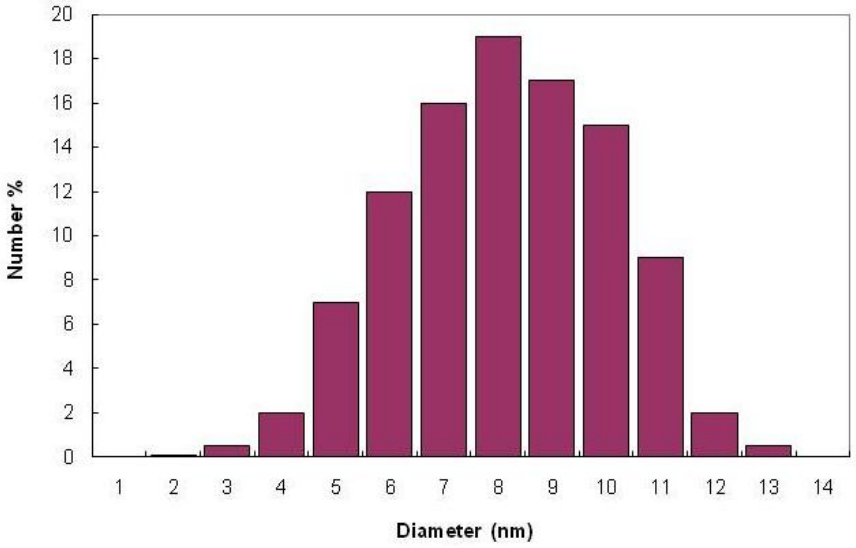

(S_5)

Figure 3. DLS diagrams of 5 MHINC samples (S_1 to S_5).

MHINC samples consisting three components with ferromagnetic properties including magnetite, hematite and zero- valent iron. Therefore, it is expected that applying an external magnetic field around the synthesis cell can control the crystal growth and the particles sizes of the synthesized ferromagnetic particles [32]. When arc is formed between two electrodes, iron plasma may be formed in the space between the two electrodes but, there is no scientific evidence in this regard. Due to the low voltage, weak arc discharge between the electrodes is established. During the process, iron is oxidized into the Fe^{2+} and Fe^{3+} ions and together with some iron atoms enter to the space between two electrodes. The presence of the magnetic field can affect on the location of iron ions and iron atoms in the crystal lattice. On the other hands, the formed nanocomposite particle is attracted by the magnetic field and removed from the space between the two electrodes. Thus, the particle growth will stop.

Based on previous reports, applying external magnetic field around the synthesis cell can change the magnetic properties of the synthesized magnetic materials [33,34]. The magnetization

saturation of all samples was studied. Fig. 4 shows magnetization curves of five samples as a function of an applied magnetic field at 273 K. Comparing of five (M-H) loops shows that all samples have similar reversibility, but the saturation of magnetization is increased when the external magnetic field is increases. Because, upon formation of Fe^{2+} and Fe^{3+} ions between anode and cathode, external magnetic field forces them to sit in the crystal lattice with a specific orientation according to the magnetic field direction. This magnetic orientation causes to synthesize a nanocomposite sample with high magnetization saturation. On the other hands, as previous reports, arrangement of ferromagnetic nanocrystals during synthesis is strongly affected via external magnetic field [35,36].

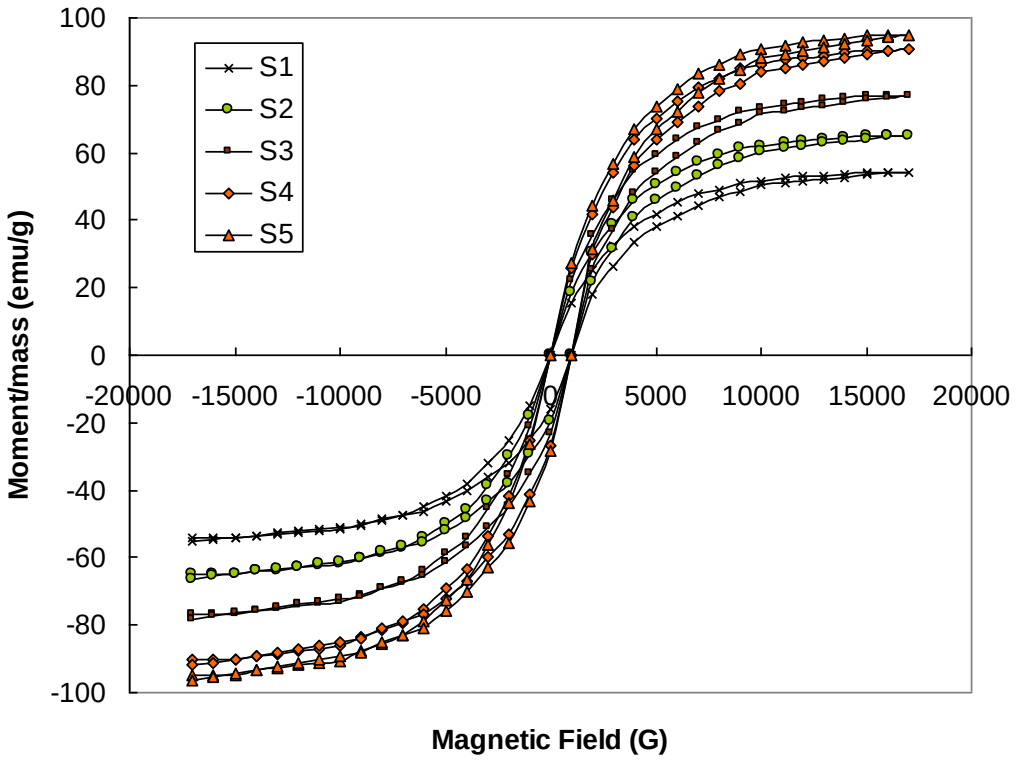

Figure 4. Magnetization as a function of an applied magnetic field MHINC samples synthesized under different power of external magnetic fields at 273 K; 0 T (S1), 0.4 T (S2), 0.8 T (S3), 1.2 T (S4) and 1.6 T (S5).

In semi-quantitative analysis by XRD, by comparing the integrated intensities of the diffraction peaks from each of the known phases, their fraction can be identified. Based on this method, the phase structure and the composition of the samples (S_1, S_4 and S_6) were characterized by XRD (Fig. 5). Synthesis 6 (S_6) was done according to S_4, but without heating before filtration. The results of phase analysis of S_1, S_4 and S_6 by XRD are summarized in Table 2. The presented results show that the presence of external magnetic field around the synthesis cell changes not only the morphology and the particles sizes of MHINC sample but also changes the sample composition. The presence of 1.2 T magnetic field considerably increases magnetite content from 39 %wt to 56 %wt by transforming of zero- valent iron while, it makes a little decrease in hematite content of the sample (from 33 %wt to 30

%wt). Upon formation of magnetite particle on the tip of electrode, magnetic field removes it from the electrode surface and attracts it. Therefore, the physical and chemical conditions for the synthesis of magnetite rather than hematite are ready.

To study the effect of heating after synthesis, the XRD patterns of samples 4 (S_4) is compared with sample 6 (S_6). In Fig. 5c, apparent peaks at 2θ of 44° and 64° indicate the transforming of zero-valent iron to magnetite meanwhile the amount of hematite remains almost the same as it is seen in Fig. 5b.

In Fig. 5b, all diffraction peaks at 2θ of 30, 36, 42, 53, 57 and 63° can be indexed as magnetite according to (JCPDS 85-1436). On the other hand, the peaks at 2θ of 33 and 54° can be indexed to α-Fe_2O_3. A part of iron content in the sample is converted into iron oxide by heating of the synthesis solution. The amount of hematite is smaller in the samples.

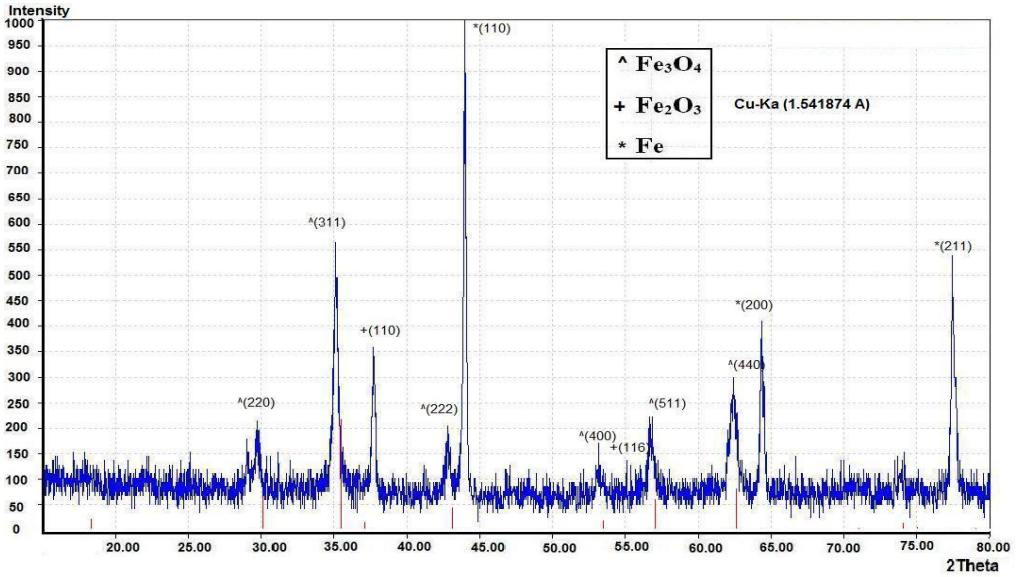

A

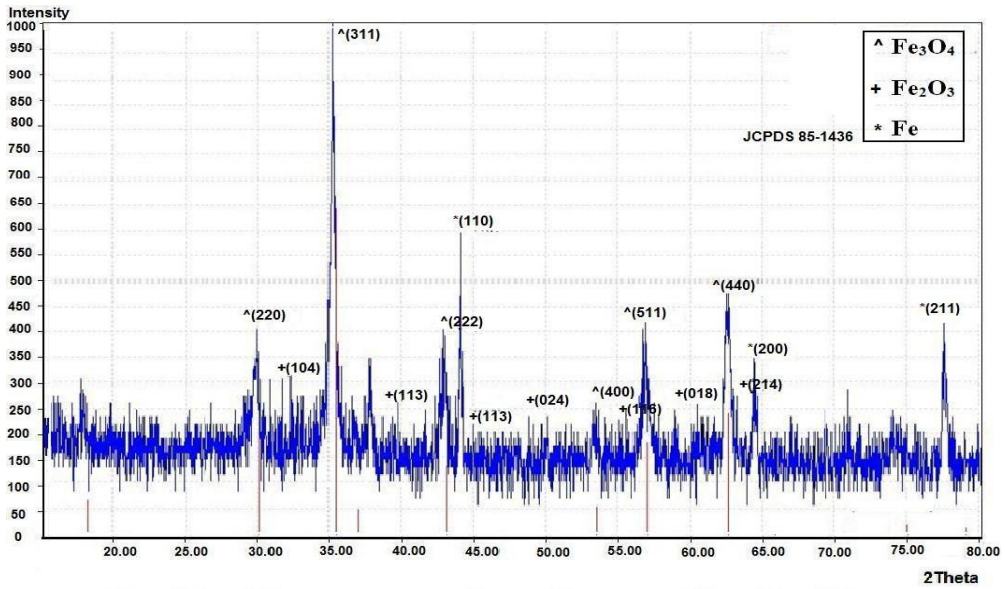

B

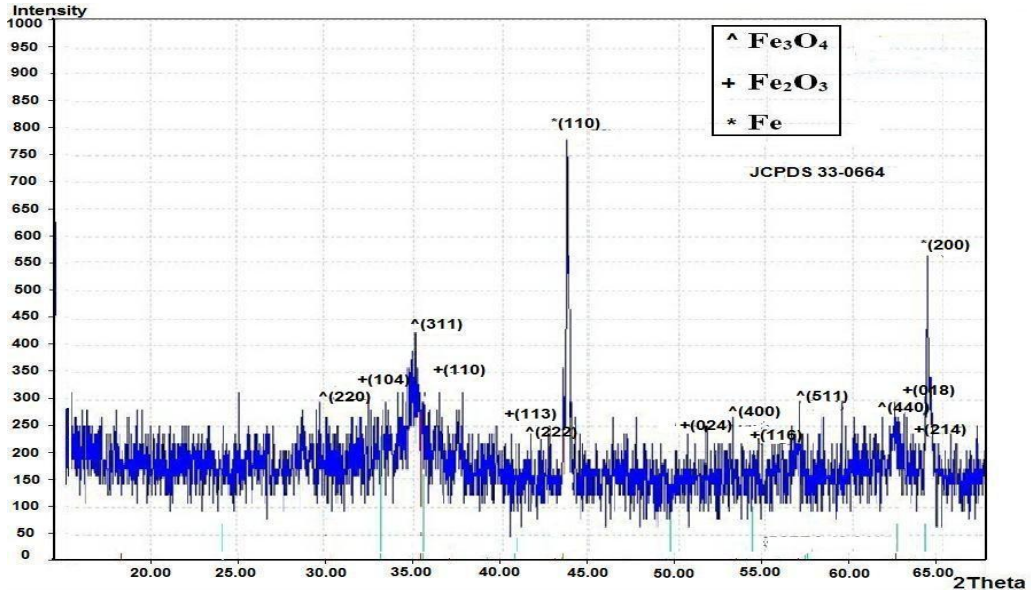

C

Figure 5. XRD patterns of MHINC samples synthesized in the different conditions; (a) without magnetic field but by heating the synthesis solution (S_4), (b) in the presence of 1.2 T magnetic filed and heating the synthesis solution and (c) in the presence of 1.2 T magnetic filed but without heating the synthesis solution.

Table 2. The phase analysis resulted by XRD patterns for MHINC samples.

Iron (%)	Hematite (%)	Magnetite (%)	MHINC Sample
29	33	39	S1
14	30	56	S4
37	28	35	S6

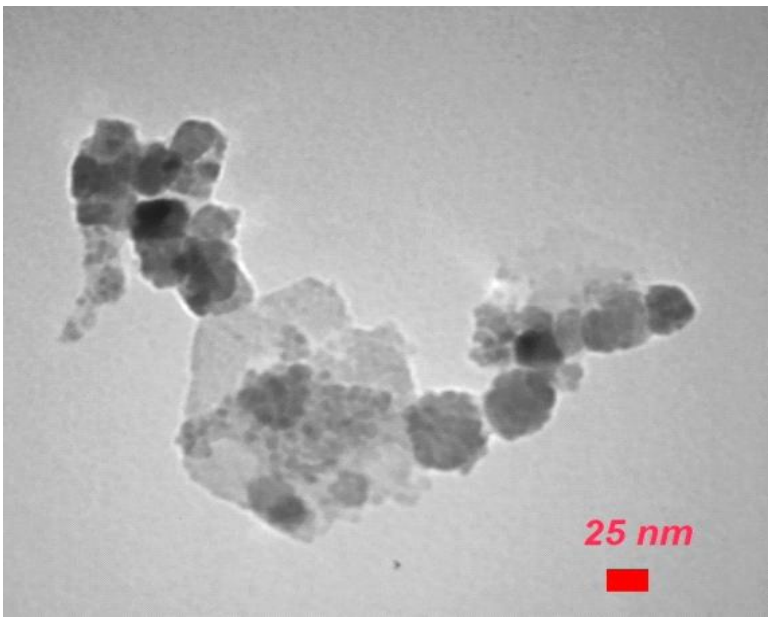

Figure 6. TEM images of synthesized MHINC sample in the presence of 3 magnets (S_4).

As the results showed, magnetic field of 1.2 T or stronger is the best choice for synthesis of MHINC. The prepared sample in the presence of three magnets (S_4) is studied by TEM (Fig. 6). TEM image shows this sample including spherical nanoparticles with a narrow range of size distribution (1-13 nm).

4. CONCLUSION

The experimental results for synthesis of magnetite/ hematite/ iron nanocomposites by electric arc discharge method showed that the applying external magnetic field had large effects on the phase transformation, particle sizes and the homogeneity of samples. By applying the magnetic field, spherical nanocomposites synthesized in the absence of magnetic field in dimension of 110-148 nm are transformed into smaller particles. In the presence of 1.2 T magnetic fields, the spherical nanocomposites with particle size in 1-13 nm are synthesized. On the other hand, the transformation of iron increased in the presence of the magnetic field.

ACKNOWLEDGEMENT
We gratefully acknowledge the financial support of this work (with project No. 89003321) by the Iran National Science Fundation (INSF) and Abhar Payame Noor University Research Council.

Referenses

1. S. N. Frank, A. J. Bard, *J. Phys. Chem.*, 81 (1977) 1484.
2. W. Weisis, D. Zscherpel, R. Schlogl, *Catal. Lett.*, 52 (1998) 215.
3. D. Bahadur, J. Giri, Bibhuti B. Nayak, T. Sriharsha, P. Pradhan, N. K. Prasad, K. C. Barick, R. D. Ambashta, *J. Phys.*, 65 (2005) 663.
4. M. Khiadani (Hajian), M. zarrabi, M. Foroughi, *Int. J. Environ. Sci. Eng.*, 11 (2013) 43.
5. Q. Li, Y.M. Xuan, J. Wang, *Exp. Therm. Fluid. Sci*., 30 (2005) 109.
6. K. Raj, R. Moskovitz, *J. Magn. Magn. Mater.*, 85 (1990) 233.
7. B.R. Pieters, R.A. Williams, C. Webb, "*Colloid and Surface Engineering Applications in the Process Industries, Butterworth-Heinemann*", Oxford, (1992) pp. 248.
8. Q. Cao, Y. Wang, J. Yu , J. Xia, C. Zhang, D. Yin, U. Hafeli, *J. Magn. Magn Mater*., 277 (2004)165.
9. C. Vestal, Z. Zhang, *Nano Lett.*, 12 (2003) 1625.
10. A. S. Teja, P.Y. Koh, *Prog. Cryst. Growth Charact. Mater.*, 55 (2009) 22.
11. S. Laurent, D. Forge, M. Port, A. Roch, C. Robic, L. Vander Elst, R.N. Muller, *Chem. Rev.*, 108 (2008) 2064.
12. D. Talapin, E. Shevchenko, H. Weller, "*Synthesis, properties and applications of magnetic nanoparticles.* In: *Nanoparticles – from Theory to Applications"*, Ed. G. Schmid, WILEY-VCH. *2nd ed.*, (2010).
13. T. Park, G. Papaefthymiou, A. Viescas, A. Moodenbaugh, S. Wong, *Nano Lett.*, 7 (2007) 766-772.
14. C. Rong, D. Li, V. Nandwana, N. Poudyal, Y. Ding, Z. Wang, H. Zeng, J. Liu, *AdV. Mater.*, 18 (2006) 2984.
15. S. Ni, X. Wang, G. Zhou, F. Yang, J. wang, Q. Wang, D. He, *Mater. Lett.*, 63 (2009) 2701.
16. K. Kalantari, M.B. Ahmad, K. Shameli, R. Khandanlou, *Int. J. Nanomedicine*, 8 (2013) 1817.
17. C.J. Choi, O. Tolochko, B.K. Kim, *Mater. Lett.*, 56 (2002) 289.

18. A.B. Chin, I.I. Yaacob, *J. Mater. Process Technol.*, 191 (2007) 235.
19. N.J. Tang, W. Zhong, H.Y. Jiang, W. Liu, Y.W. Du, *J. Magn. Magn. Mater.*, 282 (2004) 92.
20. W.S. Chiu, S. Radiman, M.H. Abdullah, P.S. Khiew, N.M. Huang, R. Abd-shukor, *Mater. Chem. Phys.*, 106 (2007) 231.
21. H. Karami, E. Chidar, *Int. J. Electrochem. Sci.*, 7 (2012) 2072.
22. H. Karami, S. Nouroozi, E. Sorbiyoon, *Nano sci. Nano technol. Ind. J.*, 7 (2013) 94.
23. K. Msellak, J.P. Chopart, O. Jbara, O. Aaboubi, J. Amblard, *J. Magn. Magn. Mater.*, 281 (2004) 295.
24. L. Hou, K.H. Zuo, Q.B. Sun, Z.M. Ren, Y.P. Zeng, X. Li, *Appl. Phys. Lett.*, 102 (2013) 082901.
25. D. Li, A. Levesque, A. Franczak, Q. Wang, J. He, J. Chopart, *Talanta*, 110 (2013) 66.
26. H. Matsushima, Y. Fukunaka, Sh. Kikuchi, A. Ispas, A. Bund, *Int. J. Electrochem. Sci.*, 7 (2012) 9345.
27. N. Sano, H. Wang, M. Chhowalla, I. Alexandrou and G.A.J. Amaratunga, *Nature (London)*, 414 (2001) 506.
28. N. Sano, H. Wang, I. Alexandrou, M. Chhowalla, K.B.K. Teo, and G.A.J. Amaratunga, *J. Appl. Phys.*, 92 (2002) 2783.
29. X.L. Fan, K.F. Yao, *Chin. Sci. Bull.*, 52 (2007) 2866.
30. C.Y. Wang, Y. Zhou, X. Mo, W. Q. Jiang, B. Chen and Z.Y. Chen, *Mater. Res. Bull.*, 35 (2000) 755.
31. H. Karami, J. Ordookhanian, A. Nezhad Ali, S. Mozaffari, *J. Magnt. Magnt. Mater.*, 379 (2015) 270.
32. R.. Chen, G. Song, Y. Wei, *J. Phys. Chem. C.*, 114 (2010) 13409.
33. Y.T. Zhou, H.L. Nie, C. Branford-White, Z.Y. He, L..M. Zhu, *J. Colloid Interface Sci.*, 330 (2009) 29.
34. W. Yantasee, C.L. Warner, T. Sangvanich, R.S. Addleman, T.G. Carter, R.J. Wiacek, G.E. Fryxell, C. Timchalk, M.G. Warner, *Environ. Sci. Technol.*, 41 (2007) 5114.
35. G.B. Khomutov, *Colloids Surf. A*, 202 (2002) 243.
36. G.B. Khomutov, S.P. Gubin, V.V. Khanin, Y.A. Koksharov, A.Y. Obydenov, V.V. Shorokhov, E.S. Soldatov, A.S. Trifonov, *Colloids Surf. A*, 198 (2002) 593.